Title	Elastic constants of GaN between 10 and 305 K
Author(s)	Adachi, K.; Ogi, H.; Nagakubo, A. et al.
Citation	Journal of Applied Physics. 2016, 119(24), p. 245111-1-245111-6
Version Type	VoR
URL	https://hdl.handle.net/11094/83930
rights	Copyright 2016 Author(s). This article may be downloaded for personal use only. Any other use requires prior permission of the author and AIP Publishing. This article appeared in Journal of Applied Physics, 119(24), 245111, 2016 and may be found at https://doi.org/10.1063/1.4955046.
Note	

Elastic constants of GaN between 10 and 305 K

K. Adachi,[1] H. Ogi,[1,a)] A. Nagakubo,[1] N. Nakamura,[1] M. Hirao,[1] M. Imade,[2] M. Yoshimura,[2] and Y. Mori[2]

[1]*Graduate School of Engineering Science, Osaka University, Toyonaka, Osaka 560-8531, Japan*
[2]*Graduate School of Engineering, Osaka University, Suita, Osaka 565-0871, Japan*

Using the antenna-transmission resonant ultrasound spectroscopy, we measured the elastic constants of GaN between 10 and 305 K using 72 resonance frequencies. The mode Grüneisen parameter is determined from temperature dependence of each elastic constant, which is larger along the c axis than along the a axis, showing anisotropy in lattice anharmonicity. The zero-temperature elastic constants, determined using the Einstein-oscillator model, yield the Debye characteristic temperature of 636 K. The *ab-initio* calculation is carried out for deducing the elastic constants, and comparison between calculations and measurements at 0 K reveals that the local-density-approximation potential is preferable for theoretically evaluating characteristics of GaN. The theoretical calculation also supports the anisotropy in lattice anharmonicity. *Published by AIP Publishing.*
[http://dx.doi.org/10.1063/1.4955046]

I. INTRODUCTION

Gallium nitride (GaN) performs a crucial role in various electric devices such as a high-electron-mobility transistor (HEMT).[1–3] The device achieves high-speed transportation of electrons known as the two-dimensional electron gas,[1,4,5] which arises from piezoelectric polarization of GaN caused by lattice strain at the epitaxial interface with another material.[5,6] Thus, the elastic constants C_{ij} of GaN are essential to estimate the performance of HEMT devices. The wurtzite GaN belongs to space group $P6_3mc$ and exhibits five independent elastic constants, C_{11}, C_{12}, C_{13}, C_{33}, and C_{44}. It is, however, difficult to accurately measure all the C_{ij} of GaN because of the limited sample size. Previously, resonance ultrasound spectroscopy (RUS),[7,8] Brillouin scattering,[9–11] and surface acoustic wave[12] were utilized for evaluating the C_{ij} of GaN at ambient temperature, but the reported values are significantly different from each other as listed in Table I. For example, the standard deviation of C_{44} exceeds 10%. Theoretical calculations were also performed,[13–16] but their agreement is poor. For example, the standard deviation of C_{66} exceeds 10% among calculations even with the same kind of atomic potential.

It is possible to predict materials properties with *ab-initio* calculation, where we need to find a suitable calculation condition (interatomic potential, cut-off energy, and so on) by comparing experimentally known properties with theoretical values, such as lattice parameters. The elastic constants are important in this process because they reflect the curvature of the interatomic potential. Thus, a calculation condition, which yields appropriate C_{ij} and lattice parameters simultaneously, is expected to provide other properties reliably. The comparison for C_{ij} requires the low-temperature measurement because the zero-temperature values are obtained in the theoretical calculation.

The low-temperature C_{ij} allows to clarify thermodynamic properties, including the Debye temperature Θ_D and the mode Grüneisen parameters γ_{ij}, which are crucial parameters of a solid: Θ_D is an essential value for characterizing its vibrational properties, and γ_{ij} indicates the strength of lattice anharmonicity. For these reasons, the measurement of C_{ij} at cryogenic temperature is scientifically and practically important, but no measured value appears for GaN.

The RUS method is a powerful tool for determining all the independent C_{ij} of anisotropic solids.[17–19] It deduces C_{ij} inversely by comparing the measured and calculated resonance frequencies. However, because high-purity and low-defect GaN specimen is limited to thin-plate shape with thickness of $\sim$400 μm (the c axis is parallel to the thickness direction),[20,21] contributions of C_{13}, C_{33}, and C_{44} to resonance frequencies become lower. As a result, it would be difficult to determine them accurately. (The RUS method with thin piezoelectric films to sandwich a specimen allows C_{ij} determination of small specimens with $\sim$1 mm dimensions[19] although it would be difficult to be applied at cryogenic temperatures.) In this study, we propose a methodology for determining the complete set of C_{ij} of a thin GaN specimen with the antenna-transmission acoustic-resonance (ATAR) method.[22] Firstly, we determine the out-of-plane elastic moduli C_{33} and C_{44} using through-thickness resonance frequencies, appearing at much higher frequency region than that used in standard RUS method. Secondly, we determine the in-plane moduli C_{11}, $C_{66}(=(C_{11}-C_{12})/2)$, and E_1, using the low-frequency resonance frequencies by fixing the measured C_{33} and C_{44} in the inverse calculation. (E_1 denotes the in-plane Young modulus.) We thus deduced all independent C_{ij} of GaN down to 10 K. We also perform *ab-initio* calculation and find that the local-density-approximation (LDA) potential shows good agreement with the measurement than the generalized-gradient-approximation (GGA) potential.

II. MEASUREMENTS

We used high-resistance wurtzite GaN, whose purity is 99.99%. (A small amount of Fe atoms ($\sim$80 ppm) was doped for trapping free carriers so that the piezoelectricity appears, allowing the excitation of vibration through the ATAR

method.) Three rectangular-parallelepiped specimens were cut out from the GaN wafer for room-temperature measurement; the typical dimensions are 3.5 mm, 3.0 mm, and 0.4 mm. (The specimen dimensions used in the low-temperature measurement are 3.500 mm, 2.994 mm, and 0.412 mm.) The mass density determined by the Archimedes method is 6.080 g/cm^3.

To cause free vibrations of the thin-plate specimen, we used the ATAR technique.[22–24] The measurement setup is illustrated in Fig. 1. We used 0.5-mm-diameter copper-wire antennas for generation, detection, and grounding, on which the specimen was located. By applying tone-burst voltage to the generation antenna, the dynamic electric field is generated near the surface, which excites various vibrational modes of the specimen via the converse piezoelectricity. The mechanical vibrations cause dynamic polarization change near the specimen surface via the piezoelectricity, which is detected by the detection antenna. The detected reverberating signals entered a superheterodyne spectrometer, and the amplitude of the driving-frequency component was extracted.[22,25] The antenna lines were attached on the heat exchanger in the cryostat, with which the specimen contacted, so that the specimen was cooled because of heat conduction through the copper antennas. The specimen temperature was measured by a semiconductor thermometer close to the specimen attached on the heat exchanger. The pressure during the measurements was kept below $\sim 1 \times 10^{-3}$ Pa.

III. RESULTS AND DISCUSSIONS

Our specimens show large aspect ratios, and bending and torsional vibrational modes principally appear in the low frequency region. Such a mode highly depends on the in-plane moduli. We then calculated the contribution of each elastic constant and piezoelectric coefficient to resonance frequencies. Figure 2 shows the normalized contributions to resonance modes up to 4 MHz for the GaN specimen used in this study. Contributions of out-of-plane moduli (C_{33} and C_{44}) are significantly smaller than those of in-plane moduli (C_{11}, C_{66}, and E_1) as expected, indicating that the out-of-plane moduli are unavailable with the low-frequency RUS method. We, therefore, determine them from the through-thickness resonance frequencies, which appear at much higher frequencies. Figures 3(a) and 3(b) show examples of measured resonant spectra for through-thickness resonances of the longitudinal wave and shear wave, respectively. Because their wavelengths ($\lesssim 0.8$ mm) are fairly smaller than in-plane dimensions (~ 3 mm), nearly plane-wave resonances appear. In this case, C_{33} and C_{44} are given by

$$C_{33} = \frac{4d^2 f_{L_n}^2 \rho}{n^2} - \frac{e_{33}^2}{\epsilon_{33}}, \tag{1}$$

$$C_{44} = \frac{4d^2 f_{S_n}^2 \rho}{n^2}, \tag{2}$$

where d, ρ, and n are thickness, mass density, and resonant mode number. e_{33} and ϵ_{33} denote the piezoelectric coefficient and dielectric constant along the x_3 direction, respectively. f_{L_n} and f_{S_n} represent nth through-thickness resonance frequencies of longitudinal and shear waves, respectively. Our previous values at room temperature[8] for $C_{33} = 389.9$ GPa and $C_{44} = 98.0$ GPa predict $f_{L_1} = 9.9$ MHz and $f_{S_3} = 14.6$

TABLE I. Elastic constants C_{ij} (GPa), the Poisson ratio ν_{ij}, and lattice parameters a and c (Å) of wurtzite GaN. The temperature coefficients $|dC/dT|$ (ppm/K) are obtained from the slopes of temperature dependences between 205 and 305 K. Zero-temperature elastic constants C_0 and mode Grüneisen parameters γ_{ij} are determined by fitting Eq. (3) to measurements.

		C_{11}	C_{13}	C_{33}	C_{44}	C_{66}	E_1	ν_{12}	ν_{13}	ν_{31}	a	c
	ATAR (present, 305 K)	359.7±0.2	104.6±0.4	391.8±0.1	99.6±0.1	114.9±0.1	300.4±0.1	0.307±0.001	0.185±0.001	0.214±0.001		
	RUS[7]	377	114	209	81.4	109	284	0.311	0.376	0.212		
	RUS[8]	359.4	92.0	389.9	98.0	115.1	303.5	0.318	0.161	0.188		
	Brillouin scattering[9]	390	106	398	105	123	325	0.320	0.181	0.199		
	Brillouin scattering[10]	374	70	379	101	134	337	0.258	0.137	0.146		
Meas.	Brillouin scattering[11]	365	114	381	109	115	300	0.305	0.208	0.228		
	Surface acoustic wave[12]	370	110	390	90	113	301	0.336	0.188	0.214		
	$|dC/dT|$ (present)	21.7	42.6	32.8	26.9	29.9	31.7	7.64	78.5	60.3		
	C_0, ν_0 (present, 0 K)	360.7	103.7[a]	393.8	100.1	115.4	301.8	0.308	0.182	0.211		
	γ_{ij} (present)	1.22	…	1.80	0.65	0.76	1.42					
	Ref. 29										3.188	5.183
	LDA (present)	369	117	402	92	107	292	0.358	0.187	0.224	3.187	5.185
	GGA (present)	328	95	354	86	100	268	0.338	0.177	0.208	3.249	5.283
	LDA[13]	396	100	392	91	126	333	0.320	0.174	0.185	3.17	5.13
Calc.	LDA[14]	350	104	376	101	115	295	0.284	0.198	0.221	3.210	5.237
	LDA[15]	334	99	372	86	101	271	0.343	0.175	0.212	3.232	5.268
	GGA[16]	329	80	357	91	110	284	0.293	0.158	0.183	3.233	5.228
	$|dC/dT|$, LDA (present)	47.1	94.7	52.5	9.9	16.7	26.7	38.1	20.9	35.0		
	$|dC/dT|$, GGA (present)	49.5	97.9	52.9	12.7	19.8	30.7	43.1	23.0	35.2		

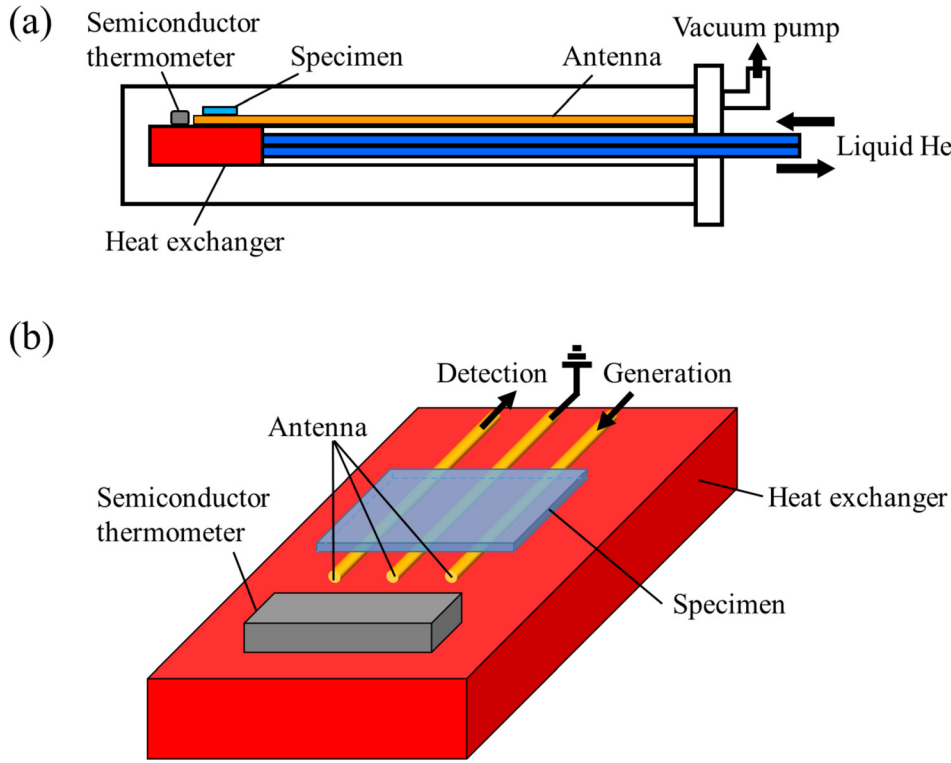[a]Average of measurements between 10 and 105 K.

FIG. 1. Setup of the antenna-transmission acoustic-resonance method for low temperatures. (a) A cross-section view, and (b) enlarged illustration near the specimen.

MHz (reported values for e_{33}[26] and ϵ_{33}[27] were used), which are close to the observations of 9.9 MHz and 14.7 MHz, respectively.

Figure 3(c) shows examples of measured resonant spectra at low frequency region. The number of detected resonance peaks is 72 at all temperatures, allowing us to make mode identification unambiguously. Using these resonance frequencies, C_{11}, C_{66}, and E_1 at each temperature are inversely determined by calculating the resonance frequencies with the Ritz method: The displacements and electric potential are expanded by linear combinations of normalized Legendre functions, involving the maximum order number of 24. C_{13} was then extracted from E_1 and other moduli. In this study, we performed the inverse calculation with fixing the piezoelectric coefficients[26] and dielectric constants[27,28] because their contributions to resonance frequencies are considerably small ($\sim$0.1%) as shown in Fig. 2. The rms error

FIG. 2. Contributions of the elastic constants and piezoelectric coefficients to free-vibration resonance frequencies ($= |(\partial f/\partial p)(p/f)|$, where p denotes each component of C_{ij} and e_{ij}) calculated for GaN specimen ($3.5 \times 3.0 \times 0.4 \, \text{mm}^3$).

between measured and calculated frequencies after convergence was less than 0.4%.

Table I shows averages of C_{ij} and the Poisson ratio $\nu_{ij} (= -s_{ij}/s_{ii}$, where s_{ij} are components of the compliance matrix) of the three specimens at 305 K together with previous measurements.[7–12] The present values agree with the recent room-temperature measurement with RUS, where larger specimens involving much higher carriers were used: The diagonal elastic constants between the present and previous measurements agree with each other within 2% difference.

At room temperature, the out-of-plane elastic constant C_{33} is higher than the in-plane elastic constant C_{11}. Because wurtzite GaN shows a hexagonal close-packed lattice, the ideal axial ratio c/a is calculated to be 1.633. However, the value deduced from the reported lattice constants[29] is 1.626, indicating a compressed structure along the c axis, making C_{33} higher than C_{11}. The Poisson ratio also reflects this characteristic structure. Because ν_{31} and ν_{13} imply the in-plane and out-of-plane softness and $C_{11} < C_{33}$, ν_{31} is larger than ν_{13}.

Figure 4 shows relative changes of C_{ij} and ν_{ij} between 10 and 305 K. Their temperature coefficients between 205 and 305 K are listed in Table I. They indicate significant anisotropy between in-plane and out-of-plane directions: C_{33} shows stronger temperature dependence than C_{11} by 34%. This causes the temperature coefficient of ν_{13} larger than that of ν_{31}; ν_{13} reflects resistance to the out-of-plane deformation when the material is uniaxially deformed in the basal plane. Thus, this highly reflects C_{33}. Similarly, ν_{31} principally reflects C_{11}. Therefore, the temperature coefficient of ν_{13} should be larger because of larger temperature coefficient of C_{33}. ν_{12} is nearly invariant or slightly increases with cooling the specimen. This is unusual property, because Poisson's ratio, which reflects compliance for deformation normal to
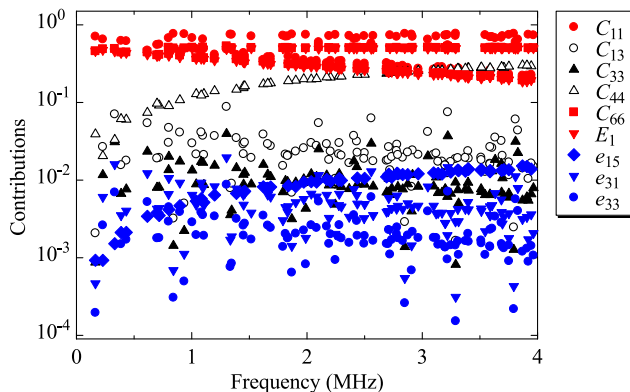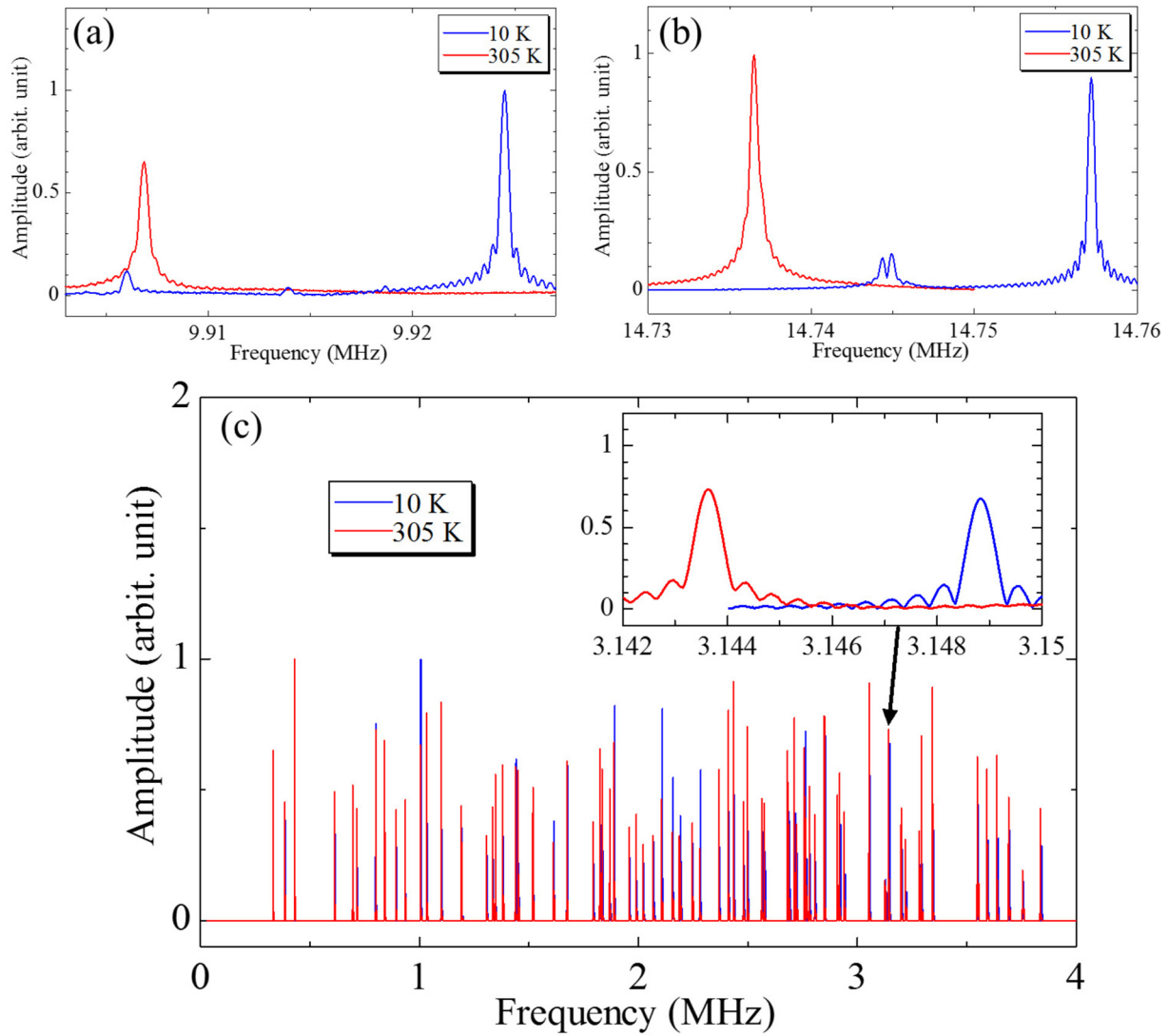
FIG. 3. (a) Through-thickness resonant spectra of the 1st longitudinal wave and (b) those of 3rd shear wave at 10 and 305 K. (c) Free-vibration resonant spectra at 10 and 305 K. Inset shows enlarged resonance peaks.

applied uniaxial stress, usually decreases as temperature decreases because of stiffness increase. ν_{12} indicates compliance for the deformation in the basal plane when the uniaxial stress is orthogonally applied in the basal plane. The applied stress also induces deformation along the c axis, but it is restricted as temperature decreases because C_{33} becomes higher more remarkably than C_{11}, and the deformation in the basal plane increases to keep minimum volume change. Therefore, the increase in C_{11} and that in C_{33} causes the opposite effect in ν_{12}, making it insensitive to temperature.

The low-temperature elastic-constant behavior is explained by the Einstein-oscillator model[30]

$$C(T) = C_0 - \frac{s}{e^{\Theta_E/T} - 1}. \tag{3}$$

Here, C_0 represents the zero-temperature elastic constant, and Θ_E is the effective Einstein temperature. Parameter s is related to the mode Grüneisen parameter γ_{ij} via[31]

$$s = \frac{3k\gamma_{ij}(\gamma_{ij} + 1)\Theta_E}{V_a}. \tag{4}$$

Here, k and V_a are the Boltzmann constant and the atomic volume, respectively. We obtained C_0 and γ_{ij} by fitting Eq. (3) to the measurements, which appear in Table I. (Because C_{13} did not follow Eq. (3), we estimated its zero-temperature value by averaging the measurements between 10 and 105 K in the plateau region.) The noticeable difference in γ_{ij} ($\gamma_{33} > \gamma_{11}$) means that lattice anharmonicity is stronger along the c axis.

We determine the Debye temperature Θ_D from C_0 using the following relationship:[32]

$$\Theta_D = \frac{h}{k}\left(\frac{3}{4\pi V_a}\right)^{\frac{1}{3}} v_m. \tag{5}$$

Here, h and q denote Planck's constant and the number of atoms in the molecule, and the mean sound velocity v_m is obtainable from C_0 using the isotropic approximation. The resultant value is $\Theta_D = 636$ K. Only one report[33] exits for the Debye temperature based on a low-temperature measurement, yielding $\Theta_D \sim 600$ K, but it estimated the value from temperature dependence of the refractive index down to
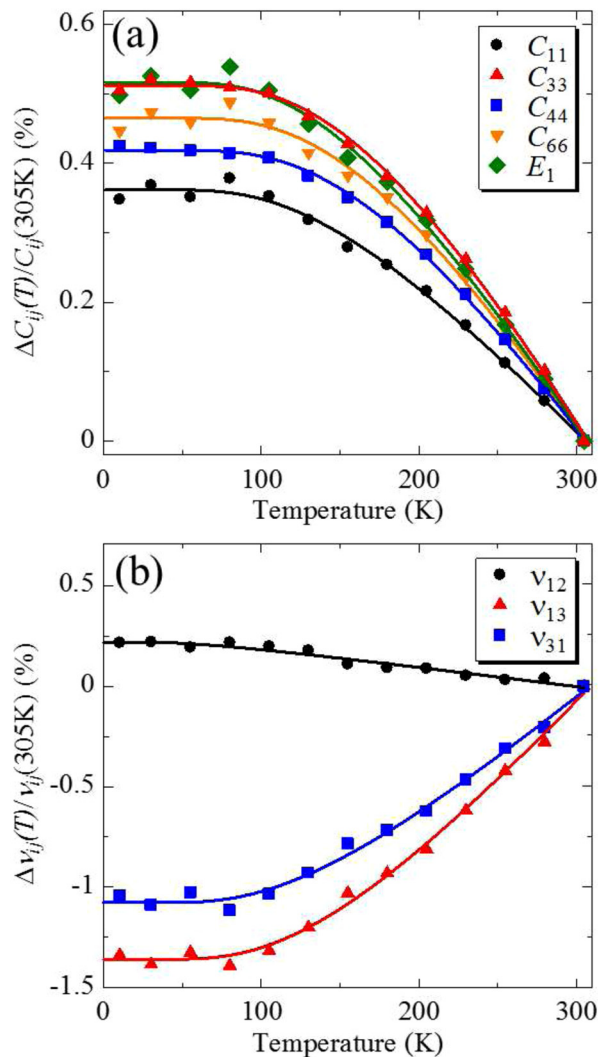
FIG. 4. (a) Temperature dependences of C_{ij} and (b) ν_{ij} of wurtzite GaN between 10 and 305 K. The solid lines in (a) show the fitted theoretical curves in Eq. (3).

77 K, where no quantum effect arises. Thus, it is obvious that our value is more reliable.

We computed the elastic constants C_{ij} of GaN with *ab-initio* calculation and compared them with our measurements. We used the density-functional theory using VASP (Vienna *ab-initio* simulation package[34]). The exchange and correlation potentials are expressed by LDA or GGA. We utilized the $10 \times 10 \times 10$ mesh k points and the plane-waves cutoff energy of 1300 eV. C_{ij} are calculated by applying various deformations with strains within $\pm 1\%$, calculating the changes of the total energy, and fitting the harmonic function.[35,36] The atoms inside cell were relaxed in the individual deformation modes. The calculated lattice parameters and elastic constants are given in Table I, together with calculated values previously reported. Our theoretical values with LDA agree with measurements both for the lattice parameters (within 0.04% error) and C_{ij} (within 8% error for the diagonal components). Therefore, it is revealed that the LDA potential is preferable for predicting materials properties of wurtzite GaN.

We then estimated the temperature dependence of C_{ij} by the *ab-initio* calculation as follows: Firstly, the cell dimensions are changed from the ground state, so as to reproduce the lattice-parameter changes caused by temperature change: We used the linear expansion coefficients (7.1 and 2.9 ppm/K along a and c axes, respectively) obtained from reported temperature dependences of the lattice constants[37] between 200 and 600 K for calculating the equivalent volume change to a set temperature. The temperature change was assumed to be within ± 1000 K, and C_{ij} at each temperature was calculated by applying up to $\pm 1\%$ strain. The results are listed in Table I. Both GGA and LDA potentials give similar temperature coefficients, and they reproduce the anisotropy in the temperature coefficient ($|dC_{33}/dT|/C_{33} > |dC_{11}/dT|/C_{11}$), supporting our measurement. This trend is attributed to anisotropy in γ_{ij} ($\gamma_{33} > \gamma_{11}$) because temperature coefficient of C_{ij} is proportional to γ_{ij}.[31]

IV. CONCLUSIONS

We measured the elastic constants of GaN at low temperatures down to 10 K using the antenna-transmission resonant ultrasound spectroscopy and determined the Debye temperature $\Theta_D = 636$ K from the zero-temperature elastic constants. The mode Grüneisen parameter along the c axis is larger than that along the a axis ($\gamma_{33} > \gamma_{11}$), displaying anisotropy in lattice anharmonicity. The *ab-initio* calculation indicates that LDA potential predicts properties more accurately than GGA potential for wurtzite GaN, and it supports the anisotropy in lattice anharmonicity.

[1]M. A. Khan, A. Bhattarai, J. N. Kuznia, and D. T. Olson, Appl. Phys. Lett. **63**, 1214 (1993).
[2]H. Xing, S. Keller, Y. Wu, L. McCarthy, I. P. Smorchkova, D. Buttari, R. Coffie, D. S. Green, G. Parish, S. Heikman, L. Shen, N. Zhang, J. J. Xu, B. P. Keller, S. P. DenBaars, and U. K. Mishra, J. Phys.: Condens. Matter **13**, 7139 (2001).
[3]R. P. Vaudo, X. Xu, A. Salant, J. Malcarne, and G. R. Brandes, Phys. Status Solidi A **200**, 18 (2003).
[4]M. Shur, B. Gelmont, and M. A. Khan, J. Electron. Mater. **25**, 777 (1996).
[5]J. P. Ibbetson, P. T. Fini, K. D. Ness, S. P. DenBaars, J. S. Speck, and U. K. Mishra, Appl. Phys. Lett. **77**, 250 (2000).
[6]R. Gaska, M. S. Shur, A. D. Bykhovski, J. W. Yang, M. A. Khan, V. V. Kaminski, and S. M. Soloviov, Appl. Phys. Lett. **76**, 3956 (2000).
[7]R. B. Schwarz, K. Khachaturyan, and E. R. Weber, Appl. Phys. Lett. **70**, 1122 (1997).
[8]N. Nakamura, H. Ogi, and M. Hirao, J. Appl. Phys. **111**, 013509 (2012).
[9]A. Polian, M. Grimsditch, and I. Grzegory, J. Appl. Phys. **79**, 3343 (1996).
[10]Y. Takagi, M. Ahart, T. Azuhata, T. Sota, K. Suzuki, and S. Nakamura, Phys. B **219–220**, 547 (1996).
[11]M. Yamaguchi, T. Yagi, T. Azuhata, T. Sota, K. Suzuki, S. Chichibu, and S. Nakamura, J. Phys.: Condens. Matter **9**, 241 (1997).
[12]C. Deger, E. Born, H. Angerer, O. Ambacher, M. Stutzmann, J. Hornsteiner, E. Riha, and G. Fischerauer, Appl. Phys. Lett. **72**, 2400 (1998).
[13]K. Kim, W. R. L. Lambrecht, and B. Segall, Phys. Rev. B **53**, 16310 (1996).
[14]K. Shimada, T. Sota, and K. Suzuki, J. Appl. Phys. **84**, 4951 (1998).
[15]Y. Duan, J. Li, S. Li, and J. Xia, J. Appl. Phys. **103**, 023705 (2008).
[16]Z. Usman, C. Cao, W. S. Khan, T. Mahmood, S. Hussain, and G. Nabi, J. Phys. Chem. A **115**, 14502 (2011).
[17]I. Ohno, J. Phys. Earth **24**, 355 (1976).
[18]A. Migliori, J. L. Sarrao, W. M. Visscher, T. M. Bell, M. Lei, Z. Fisk, and R. G. Leisure, Phys. B **183**, 1 (1993).
[19]J. Maynard, Phys. Today **49**(1), 26 (1996).
[20]K. Motoki, T. Okahisa, N. Matsumoto, M. Matsushima, H. Kimura, H. Kasai, K. Takemoto, K. Uematsu, T. Hirano, M. Ueno, D. Hara, Y. Kumagai, A. Koukitu, and H. Seki, Jpn. J. Appl. Phys., Part 2 **40**, L140 (2001).

[21]T. Detchprohm, K. Hiramatsu, H. Amano, and I. Akasaki, Appl. Phys. Lett. **61**, 2688 (1992).

[22]H. Ogi, K. Motohisa, T. Matsumoto, K. Hatanaka, and M. Hirao, Anal. Chem. **78**, 6903 (2006).

[23]H. Ogi, H. Niho, and M. Hirao, Appl. Phys. Lett. **88**, 141110 (2006).

[24]H. Ogi, Y. Tsutsui, N. Nakamura, A. Nagakubo, M. Hirao, M. Imade, M. Yoshimura, and Y. Mori, Appl. Phys. Lett. **106**, 091901 (2015).

[25]N. Nakamura, M. Sakamoto, H. Ogi, and M. Hirao, Rev. Sci. Instrum. **83**, 073901 (2012).

[26]K. Shimada, Jpn. J. Appl. Phys., Part 2 **45**, L358 (2006).

[27]D. D. Manchon, Jr., A. S. Barker, Jr., P. J. Dean, and R. B. Zetterstrom, Solid State Commun. **8**, 1227 (1970).

[28]A. S. Barker, Jr. and M. Ilegems, Phys. Rev. B **7**, 743 (1973).

[29]V. Kirchner, H. Heinke, D. Hommel, J. Z. Domagala, and M. Leszczynski, Appl. Phys. Lett. **77**, 1434 (2000).

[30]Y. P. Varshni, Phys. Rev. B **2**, 3952 (1970).

[31]H. Ledbetter, Phys. Status Solidi B **181**, 81 (1994).

[32]O. L. Anderson, J. Phys. Chem. Solids **24**, 909 (1963).

[33]E. Ejder, Phys. Status Solidi A **6**, 445 (1971).

[34]G. Kresse and J. Hafner, Phys. Rev. B **47**, 558 (1993).

[35]K. Tanigaki, H. Ogi, H. Sumiya, K. Kusakabe, N. Nakamura, M. Hirao, and H. Ledbetter, Nat. Commun. **4**, 2343 (2013).

[36]A. Nagakubo, H. Ogi, H. Sumiya, K. Kusakabe, and M. Hirao, Appl. Phys. Lett. **102**, 241909 (2013).

[37]C. Roder, S. Einfeldt, S. Figge, and D. Hommel, Phys. Rev. B **72**, 085218 (2005).